Materials Transactions, Vol. 57, No. 9 (2016) pp. 1433 to 1439
Special Issue on Advanced Materials Science in Bulk Nanostructured Metals III

Application of Al-Si Semi-Solid Reaction for Fabricating Harmonic Structured Al Based Alloy

Nur Zalikha Khalil[1,2,*], Sanjay Kumar Vajpai[3], Mie Ota[4] and Kei Ameyama[4]

[1]*Department of Mechanical Engineering, Ritsumeikan University, Kusatsu 525–8577, Japan*
[2]*Faculty of Mechanical Engineering, Universiti Malaysia Pahang, 26600 Pekan, Pahang, Malaysia*
[3]*Research Organization of Science and Technology, Ritsumeikan University, Kusatsu 525–8577, Japan*
[4]*Faculty of Science and Engineering, Department of Mechanical Engineering, Ritsumeikan University, Kusatsu 525–8577, Japan*

The present work deals with a novel approach of fabricating harmonic structure in Al alloy through the application of semi-solid reaction between Al and Si. The harmonic structured Al was prepared by powder metallurgy route, where the Al and Si powder were subjected to controlled mechanical milling followed by subsequent spark plasma sintering to make a compact. The sintered compact resulted in a network structure of hard interconnected silicon dispersed region combined with Al-Si solid solution phase, known as "shell", enclosing the soft phase of pure aluminum matrix known as "core". The harmonic structured Al compact demonstrated retention of both uniform and total elongation as compared to its heterogeneous bimodal structure counterpart, which is the typical feature of the harmonic structured material. The application of semi-solid reaction between Al and Si in fabricating harmonic structure proved to be effective in improving mechanical properties of Al alloy. Present work also discusses the deformation behavior of the sintered compacts, with respect to its strain hardening behavior.
[doi:10.2320/matertrans.MH201516]

(Received April 25, 2016; Accepted June 20, 2016; Published July 25, 2016)

Keywords: *aluminum alloy, harmonic structure, semi-solid reaction, mechanical properties, high strength, high ductility*

1. Introduction

In recent years, extensive investigations have been conducted in order to meet the demand of structural materials with superior mechanical properties, as compared to those of the conventional materials, with an emphasis on improving the existent material's properties. The improved mechanical properties will not only reduce the cost by providing small sized components with high strength but also enable the generation of novel lightweight materials for a wide range of emerging industrial applications.

Recently, Ameyama and co-workers have proposed a microstructural design to improve mechanical properties by obtaining both high strength and high ductility in metallic materials, through the formation of so-called "harmonic structured material"[1–13]. Essentially, it is an exquisite heterogeneous microstructural design, consisting of bimodal grain size distribution, in which ductile coarse grained regions (termed as "core") are enclosed in a continuously connected three-dimensional networks regions with high strength ultra-fine grained structure, known as "shell". It has been reported that a variety of metals and alloys with such structure demonstrate excellent combination of strength and ductility, when compared to its homogeneous counterpart.

It is well known that there are several strengthening mechanisms in metallic materials, such as grain refinement strengthening, solid solution strengthening, dispersion strengthening and dislocation strengthening. With regard to harmonic structured material, it was revealed that the effective strengthening mechanism is the grain refinement strengthening. In conventional harmonic structured material, ultra-fine grained structure at the "shell" region is achieved through the severe plastic deformation (SPD) process of metallic powder, via controlled mechanical milling process. The severely deformed powder exhibited heterogeneous microstructure, which has fine grained structure at the "shell" region and coarse grained structure at the "core" region.

Considering the improved ductility in harmonic structured material, in earlier works,[9,14] it has been experimentally demonstrated that an improvement in the ductility is attributed to the large uniform deformation under tensile loading. In other words, strain hardening is kept to larger strain region, and thus resulting in the improvement of ductility. Through multi scale finite element analysis (FEA), Yu *et.al.*[15] have validated that the existence of the network in the harmonic structured materials results in the avoidance of plastic deformation localization leading to homogeneous deformation behavior.

In the present work, an attempt has been made to explore the possibility to fabricate harmonic structured material through a novel approach, namely by semi-solid reaction. By utilizing the harmonic structure concept, an attempt has been made to fabricate a network structure of soft phase, which is enclosed by three dimensional interconnected network regions of hard phase. In the proposed approach, attempt has been made to design the "shell" region with a different strengthening mechanism than that of the conventional harmonic structured material, while maintaining the "core" region as the softer phase.

As described earlier, strengthening mechanism of the typical harmonic structured material relies on the grain refinement via SPD during controlled mechanical milling. However, with regard to aluminum alloy, the formation of fine grains via mechanical milling and/or retention of the same during subsequent sintering is rather difficult to achieve due to the low melting point of aluminum. Therefore, it is expected that by applying semi-solid reaction between Al and Si, it will provide another strengthening alternative to the "shell" region in harmonic structure of this alloy. In particular, it is antici-

*Graduate Student, Ritsumeikan University. Corresponding author, E-mail: daisyrose87@yahoo.com

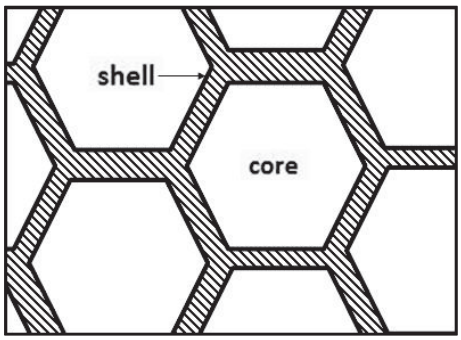

Fig. 1 Schematic of harmonic- structured design.

pated that the formation of Al-Si solid solution phase combined with dispersion of Si particles will provide two strengthening mechanisms, namely, solid solution strengthening and dispersion strengthening. Hence, by applying the semi solid reaction, it is expected that alternative and multiple strengthening mechanisms on the "shell" region of the harmonic compact Al alloy can be achieved.

In particular, by applying the semi-solid reaction of Al and Si, an attempt has been made to form a "shell" region with the above mentioned strengthening mechanism, while maintaining the "core" region as the ductile pure aluminum phase (Fig. 1). Apart from its hard nature, Si has been chosen as the secondary element candidate, because aluminum and silicon form a simple binary eutectic system and the formation of possible phases is relatively easier to characterize.

Therefore, present work has two main objectives; (1) to investigate the possibilities of formation such design in Al alloy and (2) to evaluate whether or not the harmonic structure fabricated by semi-solid reaction of Al and Si, is effective in improving mechanical properties of Al alloy in the similar manner as in the conventional harmonic structure material. In this work, the harmonic structure is fabricated through powder metallurgy route, which comprises of controlled mechanical milling of aluminum and silicon powder, followed by consolidation by spark plasma sintering (SPS) at eutectic temperature. Mechanical milling was employed to achieve uniform distribution of Si around Al particles. Finally, the deformation behavior of sintered compacts is also presented and discussed.

2. Experimental Procedures

In the present work, commercially pure Al powder prepared by plasma rotating electrode process (PREP) and pure Si powder were used as starting material. The chemical composition of the as received Al powder is shown in Table 1. Figure 2 shows the morphology of as received Al and Si powders. It can be noted that as received Al powder has smooth surface with spherical morphology, as shown in Fig. 2(a). It is also noted that the Al particles have more or less uniform particle size, which is the typical characteristic of PREP powder. The average particle size of the Al powder particles is 283 μm. As received Si powders demonstrate an irregular morphology with a wide range of particle size as shown in Fig. 2(b). The mean particle size of Si particles is 11 μm.

The mixture of aluminum and silicon powder was subjected to controlled mechanical milling using Fritch P-5 planetary ball mill, under Ar atmosphere at room temperature. A constant rotation of 150 rpm and a total time of 36 ks were used to mill the powders and the ratio of the grinding ball to powder mixture was 10: 1 by mass. WC-Co vial and high carbon chromium steel balls (SUJ2) of 3 mm in diameter were used as grinding media. Stearic acid ($C_{17}H_{35}CO_2H$) in 1.0 mass% of the total powder mass was used as process control agent to minimize the agglomeration/sticking amongst Al powders and to the milling media. The silicon content was varied from 0~5 mass% of the total powder mass during mechanical milling. Subsequently, the milled powder was subjected to spark plasma sintering under 50 MPa for 1.8 ks (0.5 h) at 850 K. Phase and microstructural characterization of sintered compacts was carried out by the means of SEM equipped with EBSD and EDS detectors. The mechanical properties of the sintered compacts were evaluated by Vickers indentation and tensile tests. The tensile specimens were prepared with a gauge length of 3 mm, width of 1 mm and thickness of 1 mm. The initial strain rate for tensile tests was 2.7×10^{-3} s^{-1} at room temperature.

Table 1 Chemical composition of as received Al powder.

Element	Si	Fe	Cu	Ti	Al
Mass (%)	0.07	0.14	0.01	0.01	Bal.

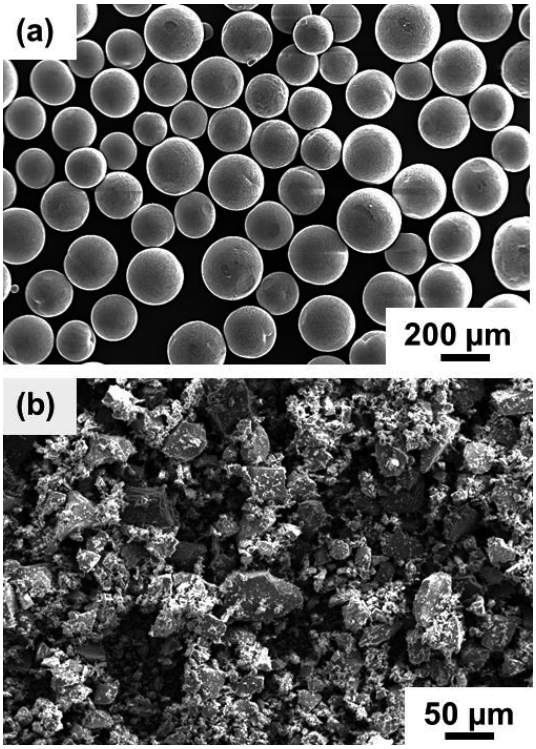

Fig. 2 Morphology of as received (a) Al powder and (b) Si powder.

3. Results and Discussions

3.1 Characterization of mechanically milled powders

Figure 3 demonstrates the morphology of the mechanically milled (MM) Al-5 mass% Si powder. After mechanical milling is conducted, the MM powder retains more or less its ini-

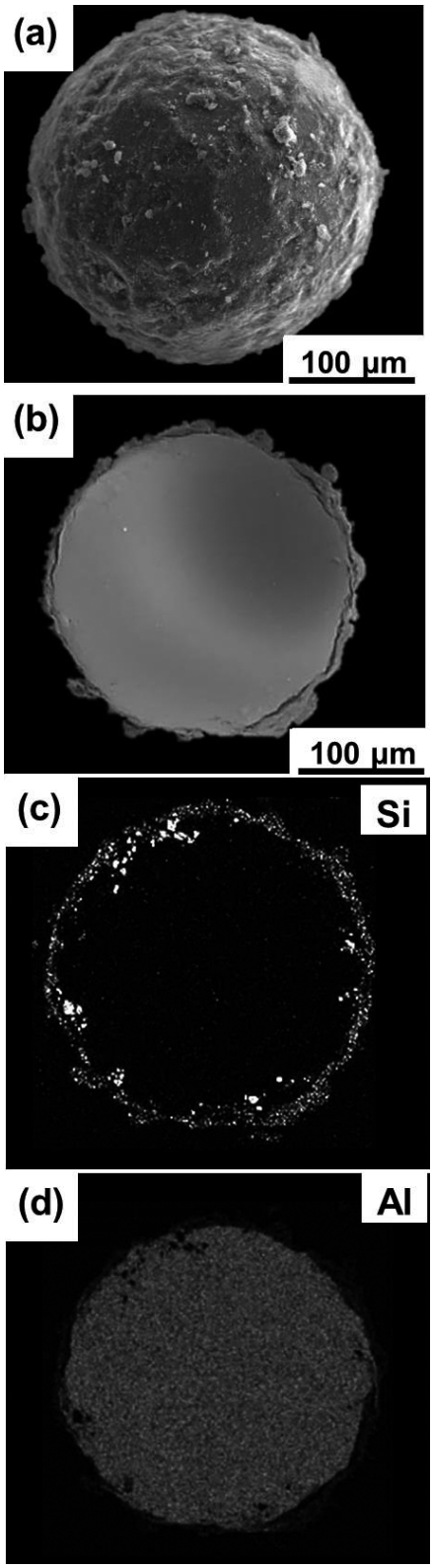

Fig. 3 SEM micrograph of the MM Al-5 mass% Si powder (a) Morphology (b) Cross-sectional image (c) and (d) are EDS results illustrating distribution of Si and Al elements, respectively.

tial shape without any appreciable deformation, as shown in Fig. 3(a). It is worth emphasizing that, this is due to the optimization made to mechanical milling parameters and condition, so that it will not lead to any agglomeration and/or sticking and fractures of the Al particles. Moreover, it can also be observed that the Al powders' surface demonstrates the formation of a deformed rough surface. This suggests that plastic deformation was induced while mechanical milling was conducted. It appears that the plastic deformation is only limited to the surface of the powder particles. Similar morphological observations have been reported also in literature[9,12,13]. Moreover, it is also noticed that the Si particles have fragmented to significantly smaller particle size after mechanical milling. As shown in Figs. 3(b)–(d), in the MM powder, Si particles are uniformly distributed around Al particles, indicating that the anticipated uniform distribution of Si particles around Al particles has been achieved at this stage.

Table 2 Vickers hardness of initial and MM Al-5 mass% Si powder.

Powder	Hardness (HV)	
	Surface	Centre
Initial Powder	27.3 ± 3	
MM 36 ks	39.9 ± 5	34.6 ± 3

Table 2 shows the average hardness values of initial and MM Al-5 mass% Si powders. The indentation was made at 98.07 mN for 5 seconds of holding time. The measurements were taken in two separate regions namely, surface and center region. For surface region, the measurements were conducted approximately 25 μm from the surface of Al particles. Meanwhile, for center region, the measurements were taken at the center of the respective particles. The measurement was made at different powder particles for each region to avoid any possible work hardening effect due to indentation. Apparently, the average hardness of both center and surface region of MM powder particles was significantly higher than that of the initial powder particles. The increment of hardness in the MM powder particles can be attributed to the work hardening effect, which is caused by the plastic deformation due to mechanical milling. Considering the increment in the average hardness value in the center region of the MM powder as compared to the initial powder, it is apparent that the work hardening effect is not only limited to the surface area of the MM powder, but also extends to some extent to the center region as well. Furthermore, in the MM powder, it can also be observed that the hardness of surface region is higher than that of the center region. It is worth emphasizing that the higher average hardness value of the surface region, as compared to that of the center region in the MM powder, reflects that the work hardening is relatively higher at the powder surface as compared to the center region. Similar observations have been reported in the other works also[11]. Moreover, the existence of Si particles on the surface region also contributes to hardness increment in surface region by acting as obstacles to dislocation movement.

3.2 Microstructural characteristics of the sintered harmonic Al compact

Figure 4 shows the BSE image of the sintered Al-5 mass% Si harmonic compact and EDS mapping images at the same magnification. Apparently, the BSE image reveals that the sintered compact demonstrates a formation of continuous network structure of two phases; dark phase in the "shell" re-

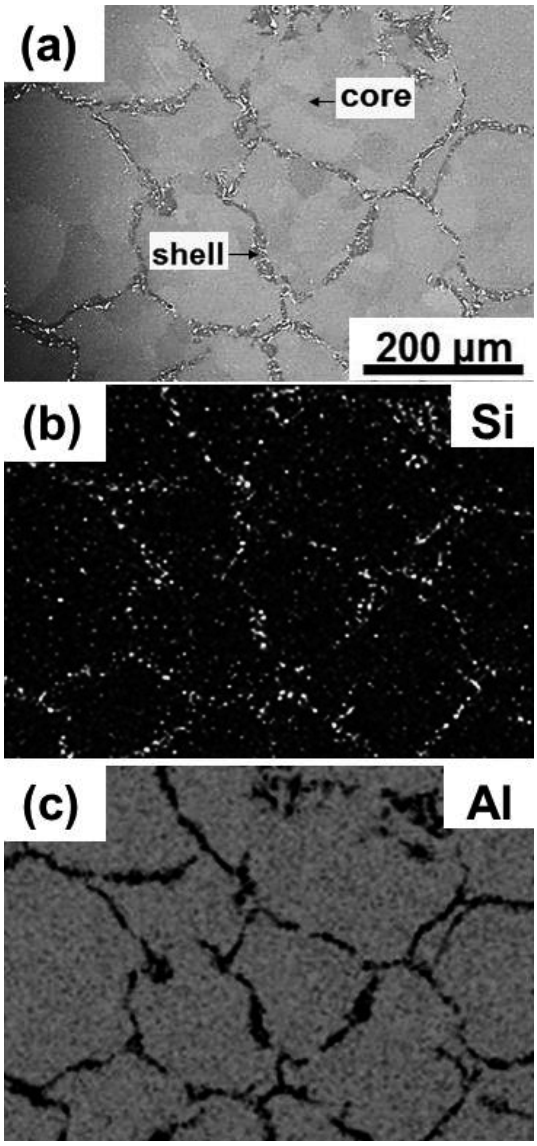

Fig. 4 Phase distribution in the sintered Al-5 mass% Si harmonic structured compact (a) BSE image (b) and (c) are EDS analysis results showing the distribution of Si and Al elements respectively.

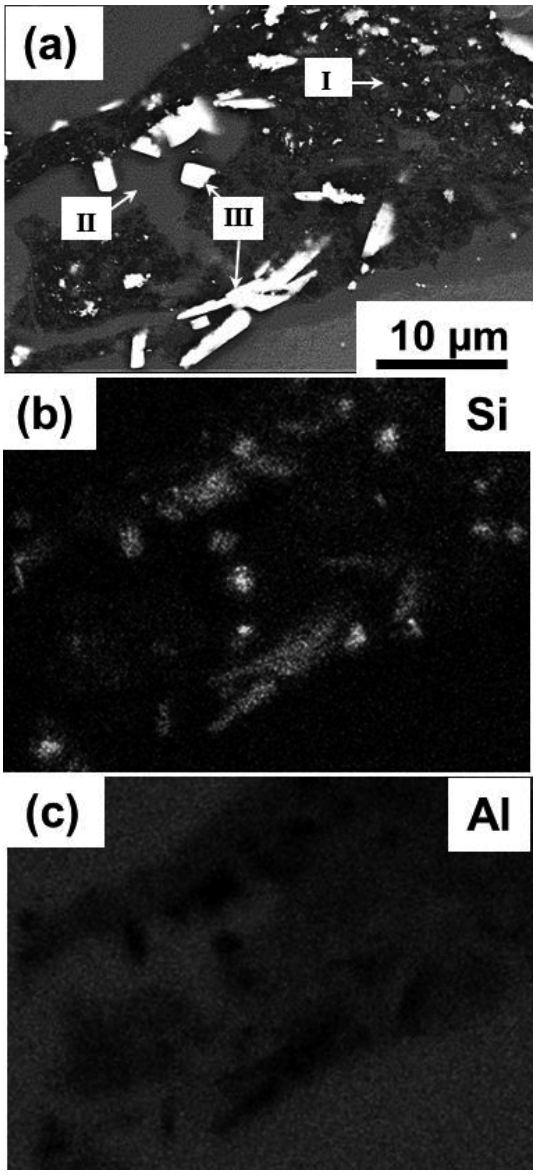

Fig. 5 Enlargement of the "shell" area for harmonic structured compact (a) BSE image of the shell region showing the presence of three main phases (b) and (c) are EDS analysis results illustrating the distribution of Si and Al elements respectively.

gion and grey phase in the "core" region, as shown in Fig. 4(a). The EDS analysis result demonstrates that the "shell" region corresponds to Si-rich region (Fig. 4(b)) while the "core" region corresponds to Al rich region (Fig. 4(c)). At this stage, it is worth emphasizing that the formation of desired harmonic structure consisting three- dimensional network of interconnected silicon dispersed region surrounding isolated aluminum matrix region has been achieved. Figure 5 depicts an enlargement of the "shell" region in the harmonic compact. From BSE image, it is observed that mainly three phases exist in the "shell" region. They are present as dark phase (area "I"), grey phase (area "II") and white phase (area "III"). These areas are marked as "I", "II" and "III" respectively in Fig. 5(a). From Figs. 5(b)–5(c), it is revealed that area "I" corresponds to the Al-Si solid solution phase (α), area "II" corresponds to pure Al while area "III" corresponds to pure silicon particles. Moreover, it is worth emphasizing that in area "III", Si particles exhibit two distinct morphologies, namely blocky particles and acicular particles, which is not presence in the initial Si powder. It has been reported elsewhere[16] that the co-existence of blocky faceted primary Si and acicular eutectic Si is a product of a hypereutectic composition during solidification. Hence, it appears that in present work the consolidation process by SPS occurs in the presence of liquid phase of hypereutectic composition in some parts of the "shell" regions. As a result, during solidification process, the liquid phase solidifies to form pure Si precipitates of different morphology, as illustrated in Fig. 5(a). From these observations, it can be concluded that, the formation of the desired harmonic structure consisting of three- dimensional network of interconnected silicon dispersed region combined with α phase (i.e: shell), surrounding isolated aluminum matrix region (i.e: core) has been achieved. In this work, the estimated "shell" fraction in harmonic structured Al compact is 15.3%.

Figure 6 shows the EBSD image quality map overlaid with grain boundaries and inverse pole figure (IPF) of the enlarge-

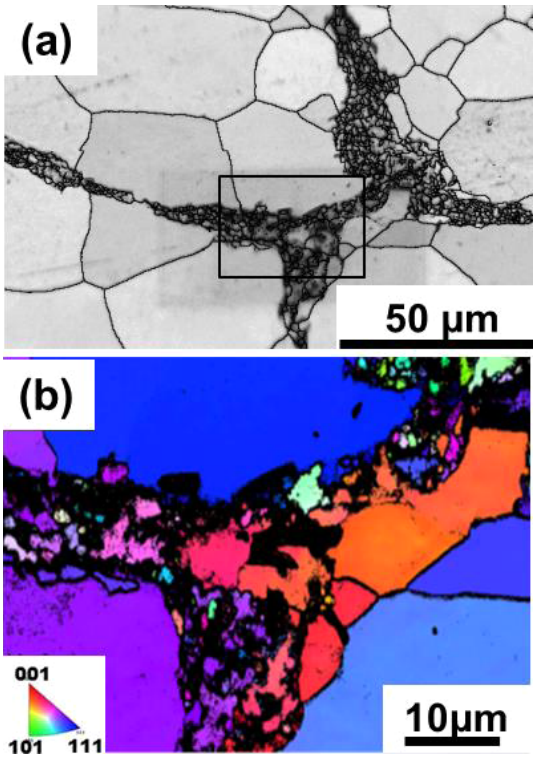

Fig. 6 Microstructure on the "shell" region for harmonic structured compact (a) EBSD band contrast map overlaid with grain boundary map (b) Inverse pole figure of the enlargement in the shell region.

ment of the "shell" region of the harmonic structure Al compact. It can be observed that, the shell region is composed of relatively fine sized grains. These fine grains are the combination of α phase grains and silicon particles.

In the harmonic structured Al compact, hardness indentations were conducted separately in the shell and the core regions, and the average hardness of the respective region was Hv: 111.9 ± 39.8 and Hv: 40.7 ± 3.1. The higher average hardness in the shell region compared to core region can be attributed to the formation of fine grain structure, α phase and the existence of Si particles.

3.3 Tensile properties of sintered compacts and its deformation behavior

In the present work, the variation of Si content during mechanical milling implies the completeness of network structure formation in the final sintered compact, in such that the increasing Si content results in a complete network structure. In this work, the variation of silicon content results in three hard phase fraction h_f, namely, 0%, 2.5% and 15.3%. In this work, the term "hard phase" is used to define the combination of Si dispersed region and α phase, while the term "shell" is used to describe the continuous network structure of the hard phase in the harmonic structured Al compact as discussed in 3.2.

Figure 7(a) shows the microstructure of the compacts with zero percent hard phase fractions, h_f. This compact refers to initial Al powder compact with no hard phase (Henceforth referred as homogeneous compact.) Figs. 7(b)–(c) illustrate the compact with $h_f = 2.5\%$ at low and high magnifications. It is observed that this compact exhibit the heterogeneous bimodal structure without the unique network structure specific to harmonic structure (Henceforth, referred as heterogeneous bimodal compact). The average grain size of the aluminum phase for homogeneous and heterogeneous bimodal structure was estimated as 132.5 μm and 107.2 μm, respectively.

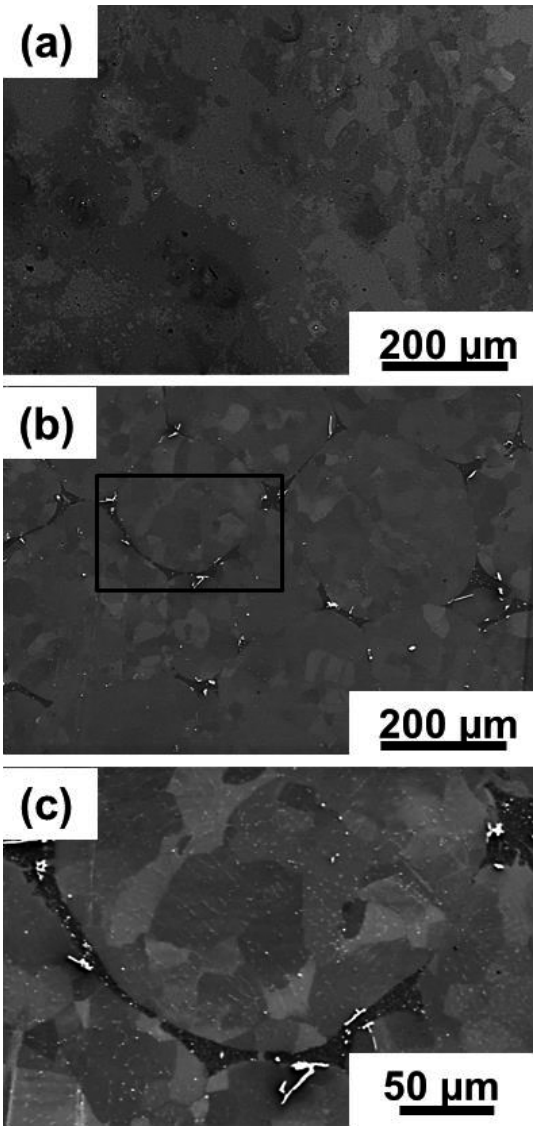

Fig. 7 Microstructure of sintered compacts at different h_f fraction. (a) Homogeneous compact, $h_f = 0\%$, (b) Microstructure of heterogeneous bimodal compact, $h_f = 2.5\%$, (c) Enlargement of the black rectangle shown in (b).

Figure 8(a) illustrates the representative nominal stress-nominal strain curves of the sintered Al compacts having different hard phase fraction, h_f. Figures 8(b)–(c) summarize the relation between stress and elongation a function of h_f. It is observed that, as compared to homogeneous compact, heterogeneous bimodal and harmonic compacts demonstrated significant increment in both 0.2% proof stress and UTS. An increment in the proof stress and UTS of these compacts appears to be related to the larger strengthening with increasing h_f, combined with the existence of fine grained structure. The general trend of variation of the tensile properties of homogeneous materials includes a decrease in ductility with increasing strength, which is related to the early plastic instability. With respect to present work, the harmonic compact is ex-

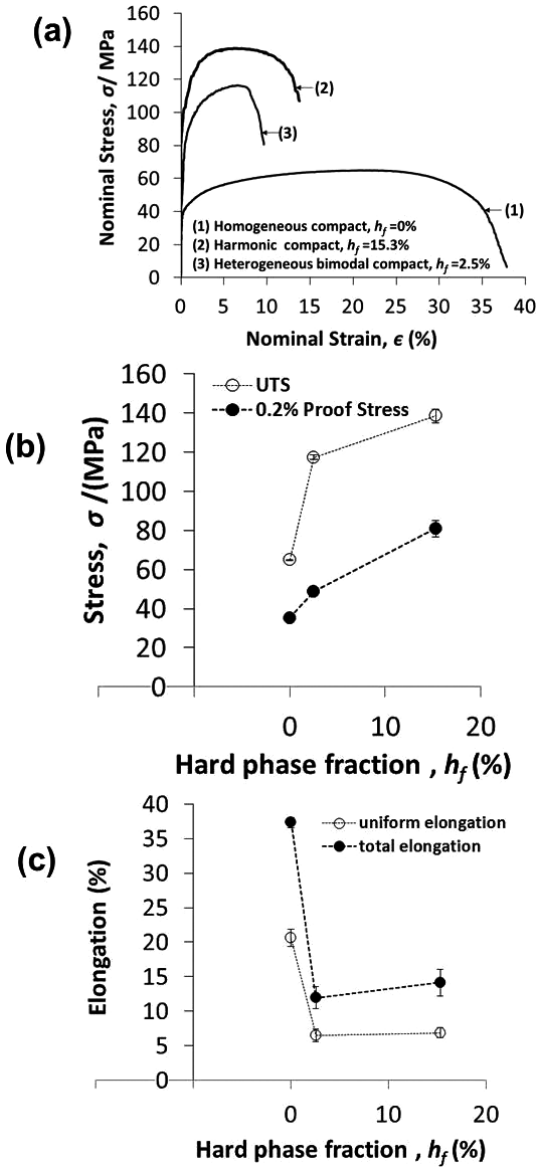

Fig. 8 Tensile properties of Al alloy samples with different hard phase fraction, h_f (a) Representative nominal stress-strain curve, (b) and (c) illustrate the correlation between hard phase fraction, h_f with stress and elongation respectively.

pected to have lower ductility as compared to that of the heterogeneous bimodal compact, due to the higher strength in the harmonic compact. Nevertheless, harmonic compact demonstrates retention in both total and uniform elongation, when compared to the heterogeneous bimodal compact. It is to mention that the retention/improvement in ductility is the typical behavior, in general, for harmonic structured material, and this is associated with the existence of unique network structure which suppresses the deformation localization specific to harmonic compact, as already mentioned in the introduction of the present paper.

To understand the deformation behavior of the harmonic structured Al compact, the true stress and true strain along with its corresponding strain hardening rate curve (SHR = $d\sigma/d\varepsilon$),was presented in Fig. 9. Essentially, in the early stage of deformation, $d\sigma/d\varepsilon$ comprise of relatively rapid decrease with increasing true strain, followed by relatively small decreasing rate, until the $d\sigma/d\varepsilon$ crosses the true stress-true strain curve at the point of plastic instability (i.e $d\sigma/d\varepsilon = \sigma$),in which the necking of the specimen starts thereafter. With regards to homogenous compact, $d\sigma/d\varepsilon$ demonstrates a relatively sluggish strain hardening rate at the early stages of deformation when compared to that of the harmonic and heterogeneous bimodal counterparts. It is worth noting that this is the typical trend in coarse grained structure. On the other hand, it is observed that the harmonic structured compact undergoes higher strain hardening at the early stage of deformation, when compared to that of its homogeneous and heterogeneous bimodal structure counterpart. It is to mention that the higher strain hardening at the early stage of deformation is a general trend for fine grained structure. When compared to the heterogeneous bimodal compact, harmonic compact demonstrated a shift of $d\sigma/d\varepsilon = \sigma$ towards a higher strain values, which indicates, in harmonic structured compact, that the point of plastic instability is delayed towards higher strain values. This implies that the plastic deformation localization is delayed, leading to the delayed necking of the specimen which results in the higher uniform elongation in the harmonic compact. Therefore, from these observations, there are two main conclusions that can be drawn for the present harmonic structured Al compact: (1) in the early stage of deformation, harmonic Al compact exhibits somewhat similar strain hardening behavior to the fine grained structure, and (2) when compared to the heterogeneous bimodal structure, the point of plastic instability $d\sigma/d\varepsilon = \sigma$ in harmonic compact is delayed to a higher strain rate, leading to improved uniform elongation in harmonic Al compact. To summarize, as compared to the homogeneous pure Al, harmonic structured Al exhibits significant improvement in the strength while retaining sufficient ductility.

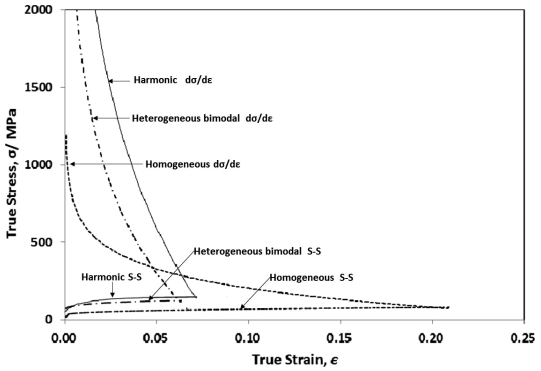

Fig. 9 True stress–true strain curves, along with their corresponding strain hardening rate (SHR) curves.

4. Conclusions

In present work, harmonic structured of Al was successfully fabricated by powder metallurgy route in which pure aluminum and silicon powder were subjected to controlled mechanical milling followed by subsequent spark plasma sintering. The mechanical performance was evaluated by tensile properties and the following conclusions can be drawn:

(1) Uniform distribution of silicon particles around Al particles can be achieved by controlled mechanical milling.

(2) Harmonic structured Al comprised of soft core areas with pure aluminum matrix, enclosed into three-dimensional network of hard Si dispersed region combined with Al-Si solid solution phase structure was successfully fabricated. The shell region of harmonic structured Al demonstrates the existence of fine grains structure. Harmonic structured Al compact demonstrates improvement in strength while retaining sufficient ductility when compared to its homogenous structure counterpart.
(3) When compared to its heterogeneous bimodal counterpart, harmonic structured Al compact demonstrates delayed plastic instability, which results in the improvement of uniform and total elongations.
(4) Network structure of three dimensional interconnected network regions of hard phase, enclosing soft phase is effective in improving mechanical properties of Al based alloy.

Acknowledgments

This research was supported by the Japan Science and Technology Agency (JST) under a Collaborative Research Based on Industrial Demand "Heterogeneous Structure Control.

REFERENCES

1) H. Fujiwara, S. Takarae and K. Ameyama: The 2nd International Symposium on Steel Science, (ISSS, 2009) pp.262–272.
2) T. Sekiguchi, K. Ono, H. Fujiwara and K. Ameyama: Mater. Trans. **51** (2010) 39–45.
3) H. Fujiwara, H. Tanaka, M. Nakatani and K. Ameyama: Mater. Sci. Forum **638–642** (2010) 1790–1795.
4) H. Fujiwara, M. Nakatani, T. Yoshida, Z. Zhang and K. Ameyama: Mater. Sci. Forum **584–586** (2008) 55–60.
5) H. Fujiwara, R. Akada, Y. Yoshita and K. Ameyama: Mater. Sci. Forum **503–504** (2006) 227–232.
6) H. Fujiwara, R. Akada, A. Noro, Y. Yoshita and K. Ameyama: Mater. Trans. **49** (2008) 90–96.
7) D. Orlov, H. Fujiwara and K. Ameyama: Mater. Trans. **54** (2013) 1549–1553.
8) O.P. Ciuca, M. Ota, S. Deng and K. Ameyama: Mater. Trans. **54** (2013) 1629–1633.
9) Z. Zhang, S.K. Vajpai, D. Orlov and K. Ameyama: Mater. Sci. Eng. A **598** (2014) 106–113.
10) Z. Zhang, D. Orlov, S.K. Vajpai, B. Tong and K. Ameyama: Adv. Eng. Mater. **17** (2015) 791–795.
11) S.K. Vajpai, M. Ota, T. Watanabe, R. Maeda, T. Sekiguchi, T. Kusaka and K. Ameyama: Metall. Mater. Trans., A Phys. Metall. Mater. Sci. **46** (2015) 903–914.
12) C. Sawangrat, O. Yamaguchi, S.K. Vajpai and K. Ameyama: Mater. Trans. **55** (2014) 99–105.
13) C. Sawangrat, S. Kato, D. Orlov and K. Ameyama: J. Mater. Sci. **49** (2014) 6579–6585.
14) S.K. Vajpai, C. Sawangrat, O. Yamaguchi, O.P. Ciuca and K. Ameyama: Mater. Sci. Eng. C **58** (2016) 1008–1015.
15) H. Yu, I. Watanabe and K. Ameyama: Adv. Mater. Res **1088** (2015) 853–857.
16) R. Asthana, A. Kumar and N. B. Dahotre: *Materials Processing and Manufacturing Science,* (Elsevier, Butterworth-Heinemann, 2006) p. 149.